Postprint of: Palacz M., Krawczuk M., An optimal form of the finite element mass matrix in the analysis of longitudinal vibrations of rods, FINITE ELEMENTS IN ANALYSIS AND DESIGN Vol. 207 (2022), 103763, DOI: 10.1016/j.finel.2022.103763

Highlights

An optimal form of the finite element mass matrix in the analysis of longitudinal vibrations of rods

Marek Krawczuk,Magdalena Palacz

- Determination of the optimal form of a rod finite element mass matrix in the context of minimal errors in calculation of natural frequencies for longitudinal vibration.
- Calculation of certain values of weights in order to determine the natural frequencies with the smallest mean error in the range of analyzed frequencies.
- Determination of optimal values of weight factors.

An optimal form of the finite element mass matrix in the analysis of longitudinal vibrations of rods

Marek Krawczuk[a,**,1] (Researcher), Magdalena Palacz[b,*,2] (Researcher)

[a]*Gdańsk University of Technology, Faculty of Mechanical Engineering and Ship Technology, Institute of Mechanics and Mechanical Engineering; Narutowicza 11/12, 80-233 Gdańsk, Poland*

[b]*Silesian University of Technology, Faculty of Organisation and Management, Department of Production Engineering; Roosevelta 26, 41-806 Zabrze, Poland*

ARTICLE INFO

Keywords:
Finite Element Method
Mass Matrix
Longitudinal Natural Frequencies
Rod Element

ABSTRACT

In this paper, an attempt is made to find the optimal form of the mass matrix of a rod finite element, which allows one to obtain the smallest errors in the longitudinal frequency determination of natural vibrations of any boundary conditions within the whole range of determined frequencies. It is assumed that the mass matrix can be treated as a linear combination of the consistent and diagonal matrices. Based on analytical considerations, the optimal values of certain weights for creating a linear combination of the mentioned matrices have been determined. As a result, a mass matrix has been obtained which allows the determination of natural frequencies with the smallest mean error within the possible spectrum of frequencies. It is also shown that the value of the weight coefficient changes depending on the number of natural frequencies within the spectrum one wants to determine.

1. Introduction

The accuracy of the Finite Element Method (FEM) can be improved using a number of methods. In practice, two main approaches can be distinguished, one related to increasing the number of finite elements of the model with the same approximation order - known as the *h-method*, or by increasing the order of the shape functions - known as the *p-method* - in Zienkiewicz and Taylor (1989), Beslin and Nicolas (1997). It has been also possible to apply a strategy based on the simultaneous increase of the number of finite elements and the order of their approximation shape functions - known as the *hpq-method*, which has been described and used by Zboiński (2010) and Zboiński (2013). Another strategy has been based on the application of functions that are the analytical solution of the shape function matrix formation problem. This approach has been practical only for one-dimensional (1D) elements as for more complicated geometries such solutions often do not exist. Certain efforts have been performed to show that a deviation from the conventional FEM formulation would benefit from an improved accuracy of results obtained by using shape functions other than polynomials Hashemi (2004).

Undoubtedly, high accuracy of numerical solutions of dynamic problems can be achieved by the use of Spectral Finite Element Method (SFEM) defined in the frequency domain Doyle (1997) or in the time domain Patera (1984). SFEM defined in the frequency domain has been based on analytical solutions of the analyzed problem and is limited to 1D problems. SFEM defined in the time domain has been a variation of a classic FEM in which an uneven distribution of nodes within an element has been applied. As a result, an almost diagonal or diagonal mass matrix can be obtained, which significantly reduces the time of numerical calculations. The fact that SFEM allows the use of approximating polynomials of high order, results in high accuracy of obtained solutions Ostachowicz, Kudela, Krawczuk and Żak (2012). Certain advantages and disadvantages of SFEM approaches have been compared and described by Palacz (2018).

It is a well-known fact that the form of a finite element mass matrix is essential for dynamic analysis. The form of a mass matrix affects both the accuracy and time of the calculations. In practice, two approaches have been developed,

*Principal corresponding author
**Corresponding author
marek.krawczuk@pg.edu.pl (M. Krawczuk); magdalena.palacz@polsl.pl (M. Palacz)
https://mostwiedzy.pl/pl/marek-krawczuk,19060-1 (M. Krawczuk);
https://www.researchgate.net/profile/Magdalena-Palacz (M. Palacz)
ORCID(s): 0000-0003-2572-7065 (M. Krawczuk); 0000-0001-8369-5175 (M. Palacz)

one using the consistent form of the mass matrix derived from the shape functions, the other using the diagonal form of the mass matrix which can be derived using the distribution of the mass and inertia between the nodes of an element. The lumped mass matrix can be obtained naturally, as is the case with SFEM in the time domain Ostachowicz et al. (2012). On the other hand, the consistent mass matrices in the case of classic FEM produce smaller errors (signifying better accuracy) in dynamic calculations with a simultaneous extension of the computation time Kim (1993).

Various forms of a consistent mass matrix of a rod finite element can be found in the literature. In Kim (1993), algebraic polynomials of different order have been used to study various matrix combinations to compare the accuracy in finite element eigenproblems. In this article, it was noticed that non-consistent mass matrices can provide more accurate natural frequencies than lumped and consistent mass formulations. While some approaches have shown excellent accuracy in lower modes, other methods have given good natural frequencies for intermediate or higher modes. The analyzed proper forms of non-consistent mass matrices have given accurate natural frequencies for both, higher and lower modes. Shape functions for superconvergent element models attained directly from the eigenvalue convergence analysis or discretization error analysis have been analyzed in the paper authored by Ahmadian and Faryghi (2011) where a new form of the mass matrix has been proposed. The method employs a series of trigonometric functions of the $\sin^2$ and $\cos^2$ type to obtain shape functions corresponding to the superconvergent element formulations. Another example of a shape function based on the $\cos + \cos^3$ trigonometric polynomial has been proposed by Stavridis, Clinckemailier and Dubois (1989) who used the polynomial for a mass matrix derivation. Their results showed that the best agreement between numerical simulations and analytical results were obtained for the $\cos + \cos^3$ shape function. For the 1D rod element, a higher-order formulation has been derived, yielding considerable accuracy improvement for the frequencies. In general, the analyzed frequency errors have been at least three times smaller than the corresponding consistent or lumped-mass formulation errors for the first two-thirds of all modes. Fried and Chavez (2004) presented the possibility of deriving the finite element mass matrix as a linear function of the parameters used for the consistent element mass matrix and the lumped element mass matrix. The authors have analyzed the convergence to the fundamental eigenvalue. An element mass matrix with which superaccurate eigenvalues have been established. This has been demonstrated for the two- and three-node rod elements.

Based on the above literature review, it has been decided to find the optimal form of a rod finite element mass matrix, which allows one to obtain the smallest errors in determining the frequency of longitudinal natural vibrations of any boundary conditions in the entire range of determined frequencies. For that purpose, it has been assumed that the mass matrix can be treated as a linear combination consistent and diagonal mass matrix of the element under investigation. Using analytical and numerical methods, the optimal weight values have been determined. These parameters allow one to determine a mass matrix for which natural frequencies have been calculated with the smallest value of the mean error in the whole possible frequency spectrum, or with the smallest relative error for a specific number of frequencies. The value of the weight factor depends on how many natural frequencies have been determined from the full spectrum and also the number of calculated frequencies.

2. Existing forms of mass matrices for a rod finite element - state-of-the-art/basic formulations

Generally, in the FEM, two types of mass matrices are utilized - the consistent and lumped. The consistent mass matrix is usually calculated from the shape functions of the finite element. For the lumped mass matrix, it is assumed that the mass and the inertia of the finite element are divided between nodes according to certain rules based on mechanical principles.

2.1. Two-node rod element

Various forms of consistent mass matrices for a rod element can be found in the literature, resulting from the expression of the assumed shape function. For two-node rod finite element Zienkiewicz and Taylor (1989) the shape functions based on a linear algebraic polynomial take the form:

$$\begin{cases} N_1 = 1 - \frac{x}{L} \\ N_2 = \frac{x}{L} \end{cases}, \tag{1}$$

where, L signifies the length of an element. For such form of shape functions, the consistent mass matrix has the following form:

$$M_C = \frac{\rho AL}{6}\begin{bmatrix}2 & 1\\ 1 & 2\end{bmatrix}, \tag{2}$$

where, ρ is the material density of the rod and A is its cross-sectional area.

Ahmadian and Faryghi (2011) proposed shape functions for the rod element based on trigonometric functions as follows:

$$\begin{cases} N_1 = cos\left(\frac{\pi x}{2L}\right)^2 \\ N_2 = sin\left(\frac{\pi x}{2L}\right)^2 \end{cases}. \tag{3}$$

For the shape functions assumed in such a manner, the element mass matrix takes the form:

$$M = \frac{\rho AL}{8}\begin{bmatrix}3 & 1\\ 1 & 3\end{bmatrix}. \tag{4}$$

Shape functions in the form of trigonometric cosine series have been used to construct the mass matrix of a rod finite element as presented in Eq.5 Ahmadian and Faryghi (2011). An illustrative comparison of the shape functions defined in Eq.1, Eq.3, and Eq.5 is shown in Figure 1.

$$\begin{cases} N_1 = \left(\frac{1}{2} + \frac{\sqrt{15}}{6}\right) cos\left(\frac{\pi x}{2L}\right)^2 + \left(\frac{1}{2} - \frac{\sqrt{15}}{6}\right) \cos\left(\frac{3\pi x}{2L}\right)^2 \\ N_2 = 1 - N_1 \end{cases}. \tag{5}$$

The element mass matrix, in this case, takes the form:

$$M = \frac{\rho AL}{12}\begin{bmatrix}5 & 1\\ 1 & 5\end{bmatrix}. \tag{6}$$

The lumped mass matrix for two-node rod finite element has the following form Ahmadian and Faryghi (2011):

$$M_L = \frac{\rho AL}{2}\begin{bmatrix}1 & 0\\ 0 & 1\end{bmatrix}. \tag{7}$$

It has been well established that such a form of mass matrix reduces the computational time for numerical calculations of dynamics problems, however, it produces a larger solution error Kim (1993).

The forms of the above presented consistent mass matrix based on trigonometric shape functions can be obtained as a linear combination of the consistent mass matrix with linear polynomial shape function and the lumped mass matrix of the rod element Fried and Chavez (2004):

$$M = (1-\varepsilon)\, M_c + \varepsilon M_L, \tag{8}$$

which leads to:

$$M = \frac{\rho AL}{6}\begin{bmatrix}2+\varepsilon & 1-\varepsilon\\ 1-\varepsilon & 2+\varepsilon\end{bmatrix}. \tag{9}$$

As it can be noticed, the mass matrix described by Eq.5 has been obtained for $\varepsilon = 0.25$, while the matrix described by Eq.7 has been obtained for $\varepsilon = 0.5$. From the literature, it follows that the matrix described by Eq.7 gives the best agreement in the case of determining the longitudinal natural frequencies of rods. It may be noted that this form gives small errors for the lowest natural frequencies of the spectrum Fried and Chavez (2004).

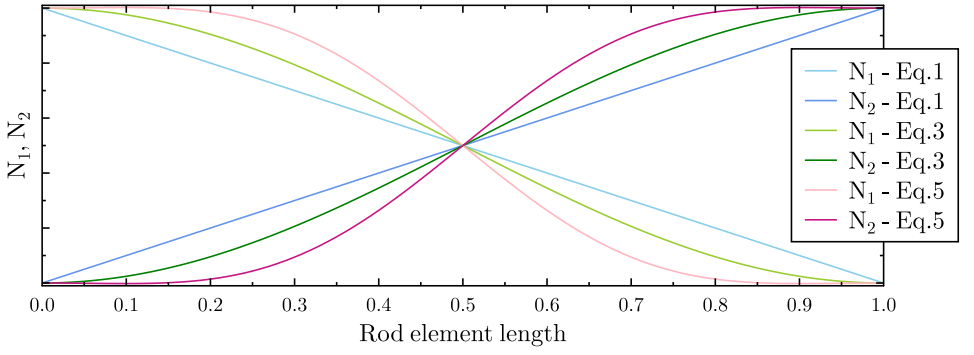

Figure 1: Shape functions of the finite two-node rod element.

2.2. Three-node rod element

For three-node bar finite elements, the most common relation describing the shape functions has the following form Fried and Chavez (2004), as illustrated in Figure 2:

$$\begin{cases} N_1 = 1 - \frac{3x}{L} + \frac{2x^2}{L^2} \\ N_2 = \frac{4x}{L} - \frac{4x^2}{L^2} \\ N_3 = -\frac{x}{L} + \frac{2x^2}{L^2} \end{cases} . \tag{10}$$

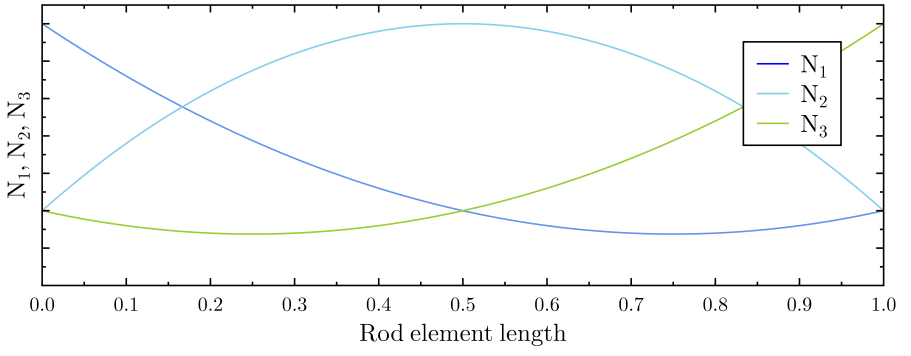

Figure 2: Shape functions of the finite three-node rod element.

The consistent mass matrix for such an element is therefore described as Dokumaci (2006):

$$M_C = \frac{\rho AL}{30} \begin{bmatrix} 4 & 2 & -1 \\ 1 & 16 & 2 \\ -1 & 2 & 4 \end{bmatrix}. \tag{11}$$

Finally, the lumped mass matrix for such an element can be described using the following relationship Fried and Chavez (2004):

$$M_L = \frac{\rho AL}{30} \begin{bmatrix} 5 & 0 & 0 \\ 0 & 20 & 0 \\ 0 & 0 & 5 \end{bmatrix}. \tag{12}$$

Additionally, for a three-node element, the mass matrix can be derived as a linear combination of the consistent mass matrix and the lumped mass matrix. In the work performed by Stavridis et al. (1989), it was shown that the best agreement between natural frequencies calculated numerically and analytically appears for $\varepsilon = 2/3$.

2.3. Four-node rod element

Shape functions for four-node rod elements have the following form Zienkiewicz and Taylor (1989), as illustrated in Figure 3:

$$\begin{cases} N_1 = 1 - \frac{11x}{2L} + \frac{9x^2}{L^2} - \frac{9x^3}{2L^3} \\ N_2 = \frac{9x}{L} - \frac{45x^2}{2L^2} + \frac{27x^3}{2L^3} \\ N_3 = -\frac{9x}{2L} + \frac{18x^2}{L^2} - \frac{27x^3}{2L^3} \\ N_4 = \frac{x}{L} - \frac{9x^2}{2L^2} + \frac{9x^3}{2L^3} \end{cases} \tag{13}$$

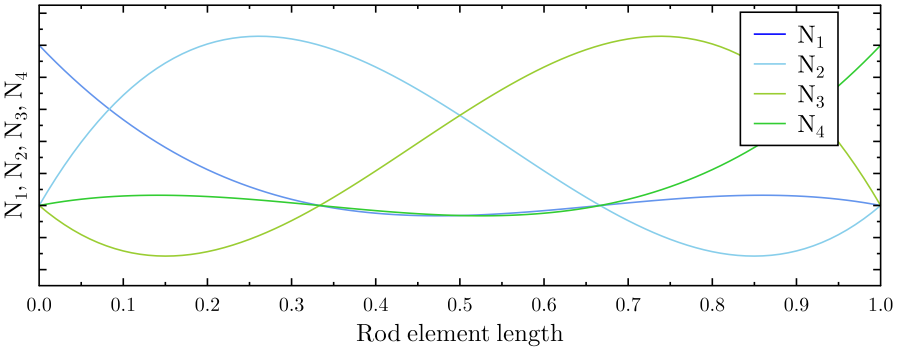

Figure 3: Shape functions of the finite four-node rod element.

Finally, the mass matrix for a four-node rod finite element, as in the previous cases, can be obtained as a linear combination of a consistent (Eq.14) and a diagonal (Eq.15) matrices with relevant matrices defined as Kim (1993):

$$M_C = \frac{\rho AL}{1680}\begin{bmatrix} 128 & 99 & -36 & 19 \\ 99 & 648 & -81 & -36 \\ -36 & -81 & 648 & 99 \\ 19 & -36 & 99 & 128 \end{bmatrix}, \tag{14}$$

$$M_L = \frac{\rho AL}{194}\begin{bmatrix} 16 & 0 & 0 & 0 \\ 0 & 81 & 0 & 0 \\ 0 & 0 & 81 & 0 \\ 0 & 0 & 0 & 16 \end{bmatrix}. \tag{15}$$

There are no studies in the literature devoted to finding the mass matrix for a four-node rod element in the form of a linear combination of consistent and diagonal mass matrices.

3. Optimal mass matrix form of a two-node rod element

To calculate the optimal form of the mass matrix, the first natural frequency of the bar modelled with rod finite elements of two-node type has been determined and compared with the analytical solution. This operation has allowed

computation of the weight coefficient ε. The calculations have been done for various rod boundary conditions, in particular fixed-fixed, fixed-free, and free-free. In the case of fixed-free boundary condition, only one two-node rod finite element has been applied, whereas for other boundary conditions two rod finite elements have been utilized. For all analyzed cases the element stiffness matrix has been assumed to follow elementary theory Zienkiewicz and Taylor (1989):

$$K = \frac{EA}{L}\begin{bmatrix} 1 & -1 \\ -1 & 1 \end{bmatrix}, \tag{16}$$

where, E is the Young's modulus of the material of which the rod is manufactured and A is the cross-sectional area of the rod.

The analytical solution of the natural frequencies of a rod depends on the boundary conditions. For a fixed-free rod, the formula for calculation of the natural frequencies takes the form Zienkiewicz and Taylor (1989):

$$\omega_k = \frac{(2k-1)\,\pi}{2L}\sqrt{\frac{E}{\rho}}, (k = 1, ..., N), \tag{17}$$

where, N is the natural frequency number, L is the length of the rod, E represents Young's modulus, and ρ is the material density.

The analytical solution for the free-free and fixed-fixed rod has the form:

$$\omega_k = \frac{k\pi}{L}\sqrt{\frac{E}{\rho}}, k = 1, ..., N. \tag{18}$$

On the other hand, the natural frequency determined numerically for a fixed-free rod, based on the assumed form of the mass matrix (Eq.9) and the elementary form of the stiffness matrix (Eq.16), has the form (for the model with one finite element):

$$\omega_1 = \frac{1}{L}\sqrt{\frac{6E}{\rho\,(2+\varepsilon)}}. \tag{19}$$

For $k = 1$, Eq.18 has the form:

$$\omega_k = \frac{\pi}{2L}\sqrt{\frac{E}{\rho}}. \tag{20}$$

By comparing Eq.19 and Eq.20, one gets

$$\varepsilon = \frac{24 - 2\pi^2}{\pi^2}, \tag{21}$$

which leads to the value of $\varepsilon = 0,4317$.

Repeating this procedure for a fixed-fixed and free-free rod, the fundamental natural frequency can be determined using two finite elements, each with a length equal to $L/2$.

$$det\left(\frac{2EA}{L}\begin{bmatrix} 1 & -1 & 0 \\ -1 & 2 & -1 \\ 0 & -1 & 1 \end{bmatrix} - \omega^2\frac{\rho AL}{12}\begin{bmatrix} 2+\varepsilon & 1-\varepsilon & 0 \\ 1-\varepsilon & 4+2\varepsilon & 1-\varepsilon \\ 0 & 1-\varepsilon & 2+\varepsilon \end{bmatrix}\right) = 0. \tag{22}$$

The non-zero root of Eq.22 takes the form of:

$$\omega_1 = \frac{1}{L}\sqrt{\frac{24E}{\rho\,(2+\varepsilon)}}. \tag{23}$$

Therefore, the analytical solution for a fixed-fixed rod (having length L, which is the same as the length of the rod in the numerical model) leads to the form:

$$\omega_k = \frac{k\pi}{L}\sqrt{\frac{E}{\rho}}, k = 1, ..., N. \tag{24}$$

By comparison of Eq.23 and Eq.24 for $k = 1$, it is possible to obtain the ε value equal to 0.4317.

Following the same procedure for a free-free rod, the ε value can be determined using a numerical model consisting of two finite elements, each of length $L/2$. The first positive, non-zero root of the characteristic equation (Eq.22) compared with the analytical solution (Eq.18) allows ε to be determined for a free-free rod. As it can be noticed, the ε value is the same for both a fixed-free and fixed-fixed rod and is equal to 0.4317.

Because the value ε is the same for all boundary conditions the optimal mass matrix has the following form:

$$M = \frac{\rho AL}{6}\begin{bmatrix} \frac{24}{\pi^2} & 3-\frac{24}{\pi^2} \\ 3-\frac{24}{\pi^2} & \frac{24}{\pi^2} \end{bmatrix}. \tag{25}$$

For the mass matrix determined in this way, the shape functions can be calculated by assuming them as:

$$\begin{cases} N_1(x) = a_1 cos\left(\frac{\pi x}{2L}\right)^2 + a_2 cos\left(\frac{3\pi x}{2L}\right)^2 \\ N_2(x) = 1 - N_1(x) \end{cases}. \tag{26}$$

The constants a_1 and a_2 are calculated based on the following assumptions:

$$\begin{cases} N_1(x=0) = 1 \\ \int_0^L N_1(x)^T N_1(x)\, dx = \frac{24L}{6\pi^2} \end{cases}. \tag{27}$$

Solving the above system of equations yields to $a_1 = 1.1093$ and $a_2 = -0.1093$. As a result, the derived optimal element shape functions take the form:

$$\begin{cases} N_1(x) = 1.1093 cos\left(\frac{\pi x}{2L}\right)^2 - 0.1093 cos\left(\frac{3\pi x}{2L}\right)^2 \\ N_2(x) = 1 - N_1(x) \end{cases}. \tag{28}$$

3.1. Numerical calculations

To compare the influence of the ε parameter value on the longitudinal natural frequency accuracy, numerical calculations were performed for a fixed-free rod made out of steel. The material parameters were assumed as follows: Young's modulus $E = 210$ GPa and density $\rho = 7860$ kg/m^3. The rod length was equal to 1 m and the cross-sectional area was equal to 0.0002 m^2. The rod was modelled with 60, two-node rod finite elements. The natural frequencies determined numerically were compared with those determined analytically according to Eq.17. For the analysis of the numerical calculation accuracy, the relative error was determined according to the following equation:

$$error = \left(\frac{\omega_a - \omega_n}{\omega_a}\right) 100\%, \tag{29}$$

where, ω_a signifies the frequency calculated analytically and ω_n signifies the frequency calculated numerically.

The results of the above-mentioned error calculations have been presented in Fig.4. On the top graph, the errors calculated for the whole range of frequencies are presented. The middle and bottom graphs present the errors calculated for a half and a quarter of the analyzed spectrum of frequencies, respectively. From the figures, it arises that the value of error depends on the number of calculated frequencies. The best results for high frequencies have been obtained for various ε values, whereas for the middle and lower frequencies, the best results were obtained for half and a quarter of the ε values, respectively.

It can be noticed from Fig.4 that the error of natural frequency calculation depends on the range of calculated frequencies. The optimal value of ε for varying ranges of calculated frequencies has been determined using the average

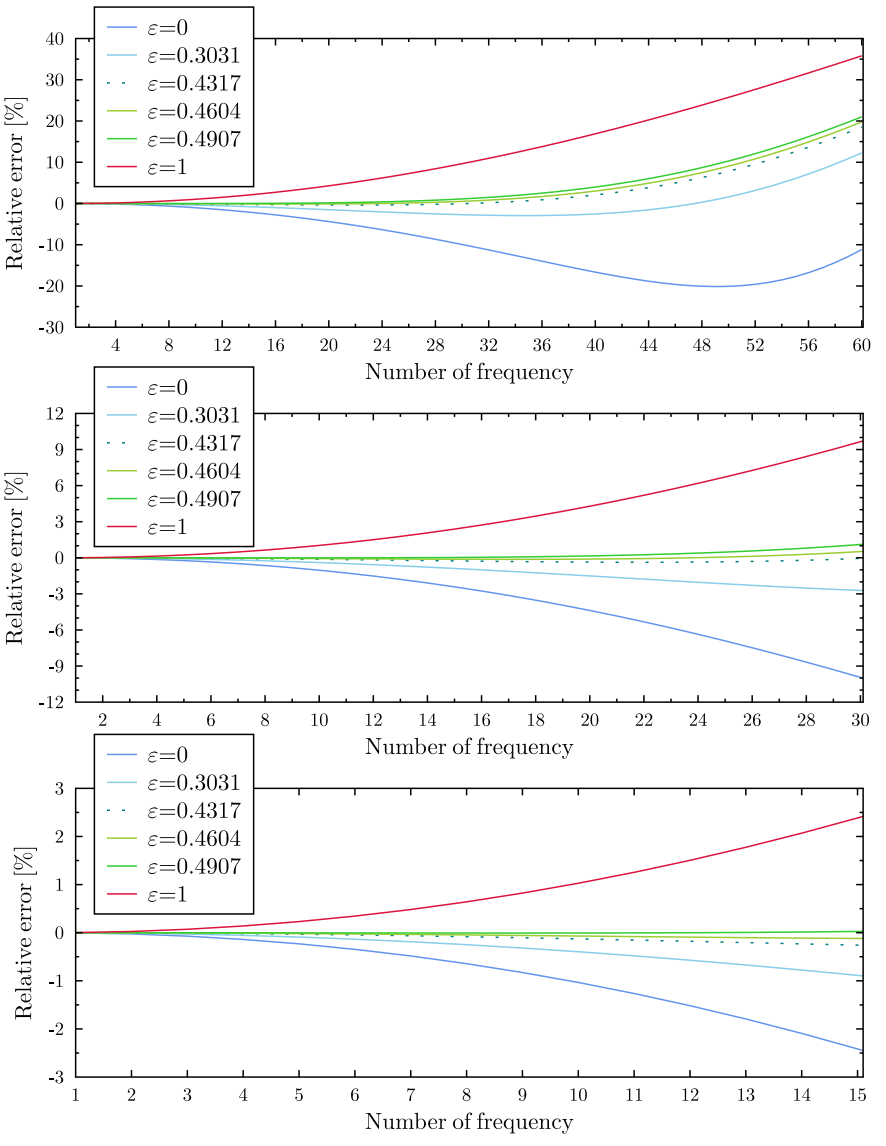

Figure 4: Relative error of the natural frequency determination of a fixed-free rod for different ranges of calculated frequencies.

error (MAE - Mean Absolute Error - an arithmetic average of the absolute errors) calculated from the following formula:

$$MAE = \frac{\sum_{i-1}^{n} |e_i|}{n}. \tag{30}$$

The following calculations have been performed for a rod with the same geometrical and material parameters as in the previous example. The simulation results for a model consisting of 40, 60, and 80 finite elements have been shown in Fig.5. In this figure, the red dashed lines mark the Nyquist (half range) and a half of the Nyquist (quarter range) frequencies in each analyzed case.

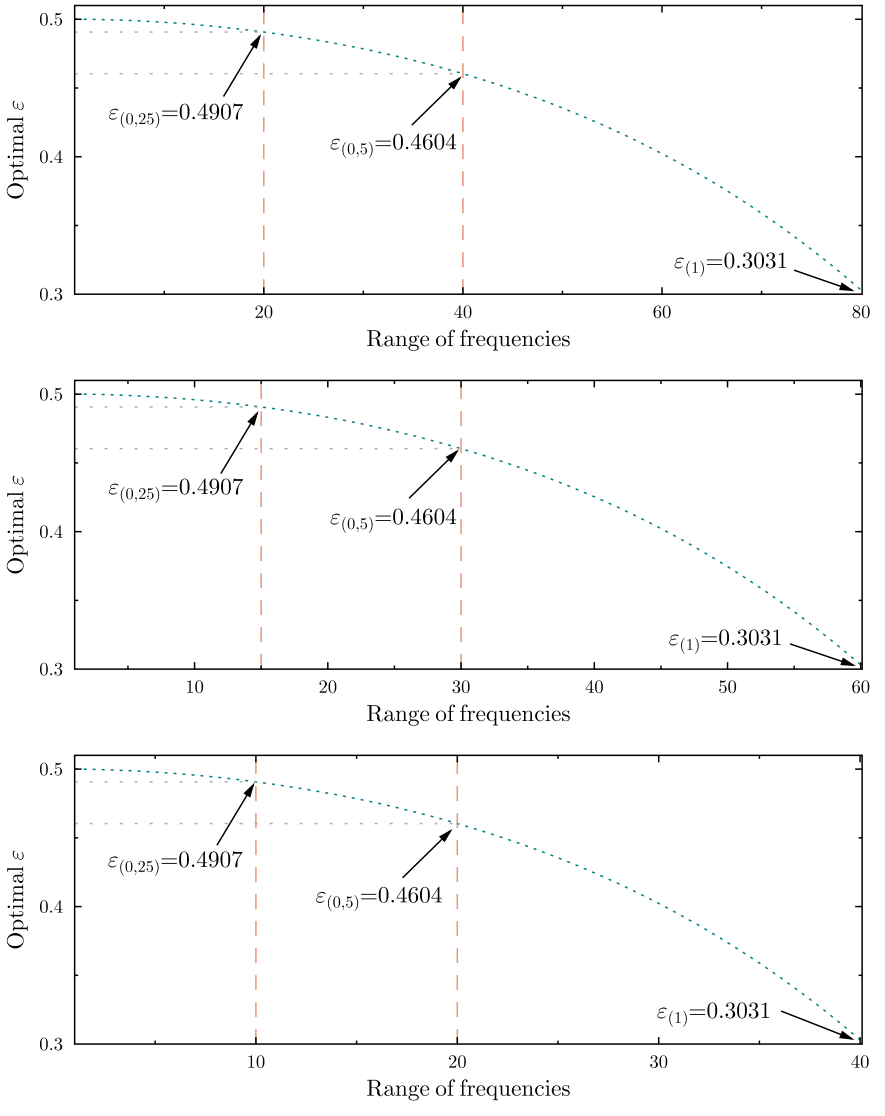

Figure 5: The ε coefficient for the natural frequency ranges of the analyzed rod - 80, 60 and 40 2-node finite elements.

Table 1
Average errors for 2-node element as a function of ε calculated for different ranges of frequencies

Range	ε=1.0	ε=0.5	ε=0.0	ε=**0.3031**	ε=**0.4604**	textbfε=0.4907
Full	12.7338	4.5307	9.9468	**2.3846**	3.7532	4.3404
Half	3.3633	0.2693	3.4450	1.1063	**0.1055**	0.2095
Quarter	0.8518	0.0161	0.8592	0.3237	0.0518	**0.0060**

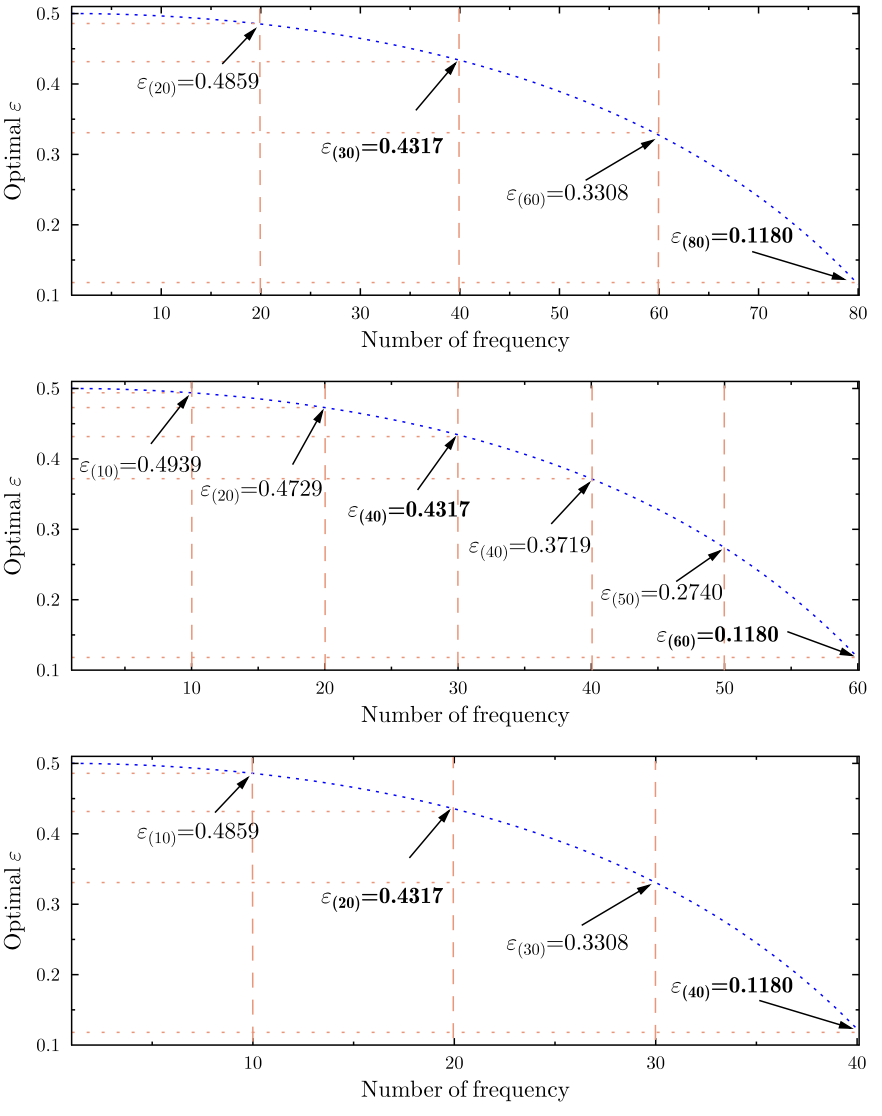

Figure 6: The ϵ coefficient for specific natural frequencies.

From the curves presented in Fig.5 it may be seen that the optimal value of ϵ has not been influenced by the total number of finite elements in the model. For the full frequency spectrum, the best correlation between analytical and numerical solutions has been obtained for $\epsilon = 0.3031$. For the half spectrum, the optimal value of ϵ is equal to 0.4604, whereas for the quarter of spectrum $\epsilon = 0.4907$. To check the influence of the boundary conditions on the value of the ϵ coefficient, analogous calculations have been performed for a free-free and fixed-fixed rod with the same geometrical and material parameters as in the previous examples. After the calculation was performed, it appeared that various boundary conditions did not influence optimal values of ϵ, therefore the illustrative figure was omitted. Additionally, for several ϵ values, the mean error for the frequency range was calculated. These results have been summarized in Table 1. The optimal ϵ, for which the average error for various frequency ranges is the smallest, have been additionally marked in Fig.5. It may be concluded that for a different range of calculated longitudinal natural frequencies, there exists a value of ϵ which allows one to obtain the smallest average error in each particular range.

Following, an optimal (in terms of minimal calculation error) value of ϵ was calculated for each frequency of the spectrum. The number of frequencies was dependent on the number of finite elements in the numerical model. The results of the calculations are presented in Fig.6. The outcomes presented in Fig6 show that for the last frequency

of the spectrum, the best results are obtained for $\varepsilon = 0.1180$, whereas for the first frequency the best agreement is achieved with $\varepsilon = 0.5$ (superconvergent element known from Kim (1993)). On the other hand, for $\varepsilon = 0.4317$ (the value proposed by Authors) the best accuracy has been obtained for the middle frequency. The change of the boundary condition type and the finite element grid density has not influenced the optimal value of ε. These observations have been confirmed by the results gathered and presented in Table 2. The table presents a set of values for the calculated relative errors of selected frequencies in the case of specified values of the ε parameter. The smallest calculated error values have been marked in bold text (on the diagonal) - as it can be noticed, these are the results for certain optimal values of ε (listed in the first row of the table), which is additionally illustrated in the middle graph of Fig.6.

Table 2
Relative errors as a function of ε calculated for specific frequencies

No	ε=0.5	ε=0.4939	ε=0.4729	ε=0.4317	ε=0.3719	ε=0.2740	ε=0.1180
1	**0.00000**	-0.00003	-0.00015	-0.00039	-0.00073	-0.0012	-0.0021
10	0.01287	**0.00030**	-0.04302	-0.12819	-0.25219	-0.45620	-0.78387
20	0.23529	0.18263	**0.00070**	-0.35914	-0.88841	-1.77320	-3.23268
30	1.28318	1.16630	0.76074	**-0.04966**	-1.26206	-3.34573	-6.9492
40	4.27997	4.08870	3.42135	2.07055	**0.00506**	-3.67808	-10.49277
50	10.67017	10.42576	9.56873	7.81330	5.07320	**0.00678**	-10.06431
60	21.38521	21.14440	20.29811	18.55543	15.80957	10.64528	**0.00564**

4. Optimal mass matrix form of a three-node rod element

To determine the optimal form of the mass matrix for the three-node rod finite element, the first natural frequency of the rod has been determined numerically and compared with the analytical solution. This operation has allowed the calculation of the weight coefficient ε for the three-node finite element. The computations have been performed for various boundary conditions (i.e., fixed-free, fixed-fixed, and free-free). In the case of the fixed-free boundary condition, only one three-node rod finite element has been applied, whereas for the other boundary conditions, two three-node rod finite elements have been utilized.

The element stiffness matrix has been assumed according to the elementary rod theory Zienkiewicz and Taylor (1989) and it can be expressed as Fried and Chavez (2004):

$$K_e = \frac{EA}{3L}\begin{bmatrix} 7 & -8 & 1 \\ -8 & 16 & -8 \\ 1 & -8 & 7 \end{bmatrix}. \tag{31}$$

The first positive and non-zero root of the eigenproblem in the case of fixed-free boundary conditions is given by the formula:

$$\omega_1 = \sqrt{\frac{52E + 3E\varepsilon + E\sqrt{9\varepsilon^2 - 168\varepsilon + 1984}}{L^2\rho\,(3 + 2\varepsilon)}}. \tag{32}$$

Comparing the above expression with the relation describing the first natural frequency of longitudinal vibrations of the rod determined analytically, the value of $\varepsilon = 0.6295$ has been obtained. The same value of ε has been also obtained for free-free and fixed-fixed rods.

For the determined value of ε, the mass matrix of the analyzed element takes the form:

$$M_e = \frac{\rho AL}{30}\begin{bmatrix} 4.6925 & 0.615 & -0.3075 \\ 0.615 & 18.77 & 0.615 \\ -0.3075 & 0.615 & 4.6925 \end{bmatrix} \tag{33}$$

4.1. Numerical calculations

As in the case of the two-node element, the changes in relative error have been first calculated for a rod element modelled using 40 three-node finite elements. The material and geometrical parameters have been assumed the same

as for the rod modelled using two-node elements. The relative error of the natural frequency has been determined according to the relation given by Eq.29. The results of the error calculations have been presented in Fig.7. On the top graph, the error value changes calculated for the whole range of frequencies are presented. The middle and bottom graphs present the error value changes calculated for a half and a quarter of the analyzed spectrum of frequencies, respectively. From the presented figures it arises that the value of relative error depends strongly on the number of calculated frequencies. Moreover, accurate results for high frequencies have been obtained for various values of ε.

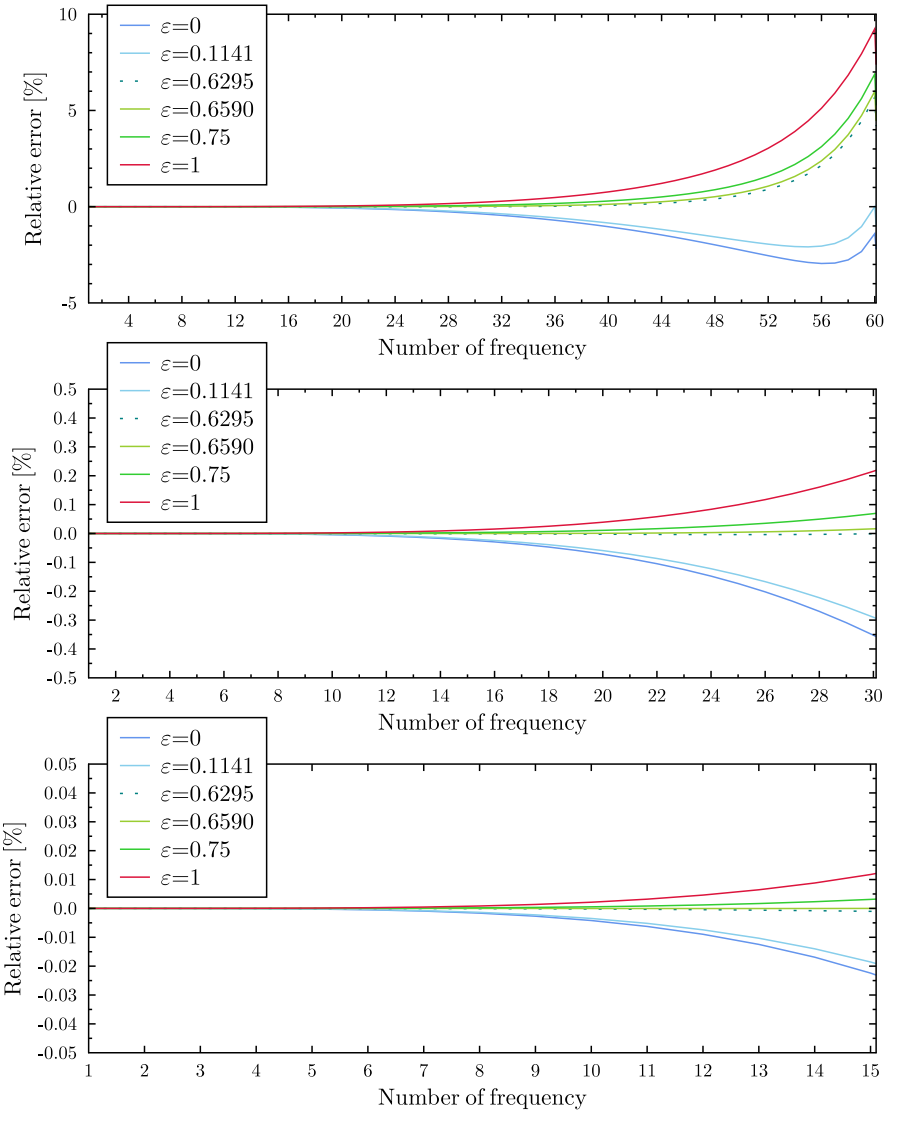

Figure 7: Relative error of the natural frequency determination of a fixed-free rod - 60, 30 and 15 three-node finite elements.

The following calculations have been performed for a rod modelled with different numbers of three-node elements (i.e., 40, 60, and 80). These calculations aimed to establish the optimal ε value. The results of the calculations are presented in Fig.8. In this figure, as in the case of the analysis for two-node rod finite elements, the red dashed lines mark the Nyquist, half of the Nyquist, and a quarter of the Nyquist frequencies in each analyzed case. It is worth noting that in all figures a drop in the middle of the analyzed spectra can be observed. This effect appears due to the periodic character of the model Żak, Krawczuk and Palacz (2016), therefore the popular conviction that such a model allows the determination of as many natural frequencies as its number of degrees of freedom (DOFs), may be misleading under

certain conditions. However, the optimal values of ε in terms of minimal average error for various frequency ranges have been calculated and those results have been gathered in Table 3. The optimal ε values, in this case, have been shown in bold text.

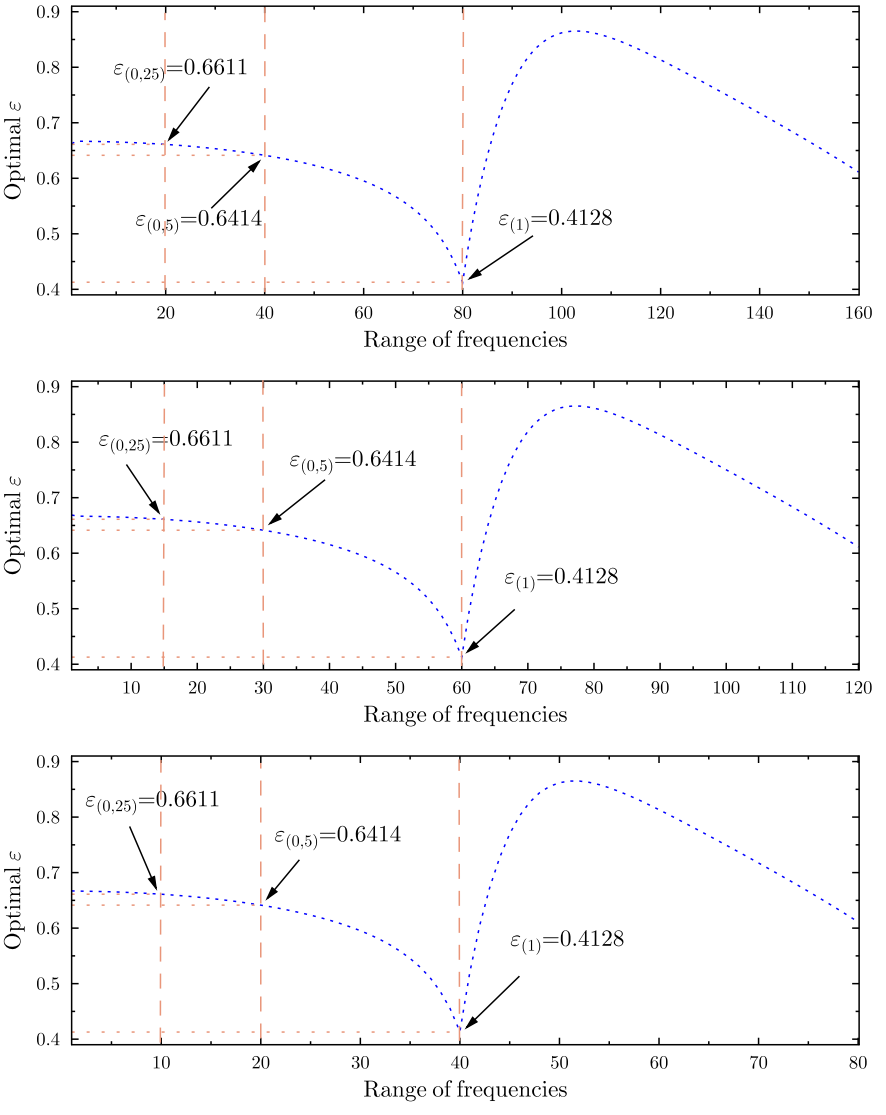

Figure 8: The ε coefficient for the natural frequency ranges of the analyzed rod - 80, 60 and 40 3-node finite elements.

Table 3
Average errors for 3-node element as a function of ε calculated for different ranges of frequencies

Range	ε=1.0	ε=0.6666	ε=0.0	ε=**0.4128**	ε=**0.6414**	ε=**0.6611**
Full	1.229	0.5330	0.8608	**0.2749**	0.4805	0.5214
Half	0.0449	0.0031	0.0775	0.0280	**0.0009**	0.0025
Quarter	0.0027	4.44e-05	0.0051	0.0019	0.0001	**1.13e-5**

Next, the optimal values of the ε coefficient for particular rod longitudinal frequencies have been determined. For this purpose, each frequency determined numerically has been compared with the respective analytical solution. The optimal value of ε has been found in regards to achieving the smallest relative error of each frequency of the spectrum (Fig.9). Similarly to the results obtained with the two-node model, the curves presented in Fig.9 show that the optimal value of ε is not influenced by the total number of finite elements in the model. For the full frequency spectrum, the best correlation between analytical and numerical solutions has been obtained for $\varepsilon = 0.1141$. For the half spectrum, the optimal value of ε (the value proposed by Authors) is equal to 0.6295, whereas for the quarter of spectrum $\varepsilon = 0.6590$. To investigate the influence of the boundary conditions on the value of the ε coefficient, analogous calculations have been performed for a free-free and fixed-fixed rod with the same geometrical and material parameters as in the previous examples. After performing the calculations, it appeared that the boundary conditions did not influence the optimal values of ε, therefore the illustrative figure has been omitted. These observations have been confirmed by the results collected and presented in Table 4. The table presents a summary of the values of the calculated relative errors at selected frequencies for specific ε values. The smallest values of the calculated errors have been marked in bold text (on the diagonal) - as can be noticed, these are the results for certain optimal values of the ε parameter (listed in the first row of the table), which is further indicated in the middle graph of Fig.9.

Table 4
Relative errors as a function of ε calculated for specific frequency - 3-node finite element

No	ε=0.6666	ε=0.6636	ε=0.6526	ε=0.6295	ε=0.5908	ε=0.5026	ε=0.1141
1	**-2.37e-10**	-5.32e-10	-9.16e-10	-2.03e-09	-3.81e-09	-8.01e-09	-2.68e-08
10	2.02e-05	**7.822e-07**	-6.90e-05	-0.00021	-0.00046	-0.0010	-0.0034
20	0.00157	0.00123	**9.02e-06**	-0.0025	-0.0068	-0.01664	-0.05924
30	0.02053	0.01877	0.01244	**-0.00083**	-0.02302	-0.07330	-0.29006
40	0.13967	0.13401	0.11370	0.07115	**0.00013**	-0.16042	-0.84616
50	0.77567	0.76107	0.70865	0.59878	0.41536	**0.00053**	-1.76592
60	6.06824	6.03755	5.92700	5.69359	5.29870	4.38018	**0.0014**

5. Optimal mass matrix form of a four-node rod element

To determine the optimal form of the mass matrix in the case of a four-node rod finite element, similarly to the previously discussed elements, the first natural frequency of the modelled rod has been determined and compared with the analytical solution. This operation has allowed the value of the weight coefficient ε to be determined. The calculations have been performed for all types of already mentioned boundary conditions (i.e., fixed-free, fixed-fixed, and free-free). In the case of the fixed-free boundary condition, only one four-node rod finite element has been applied, whereas for the other boundary conditions, two finite elements have been utilized.

The four-node element stiffness matrix has been assumed as Zienkiewicz and Taylor (1989):

$$K_e = \frac{EA}{40L}\begin{bmatrix} 148 & -189 & 54 & -13 \\ -189 & 432 & -297 & 54 \\ 54 & -297 & 432 & -189 \\ -13 & 54 & -189 & 148 \end{bmatrix}. \tag{34}$$

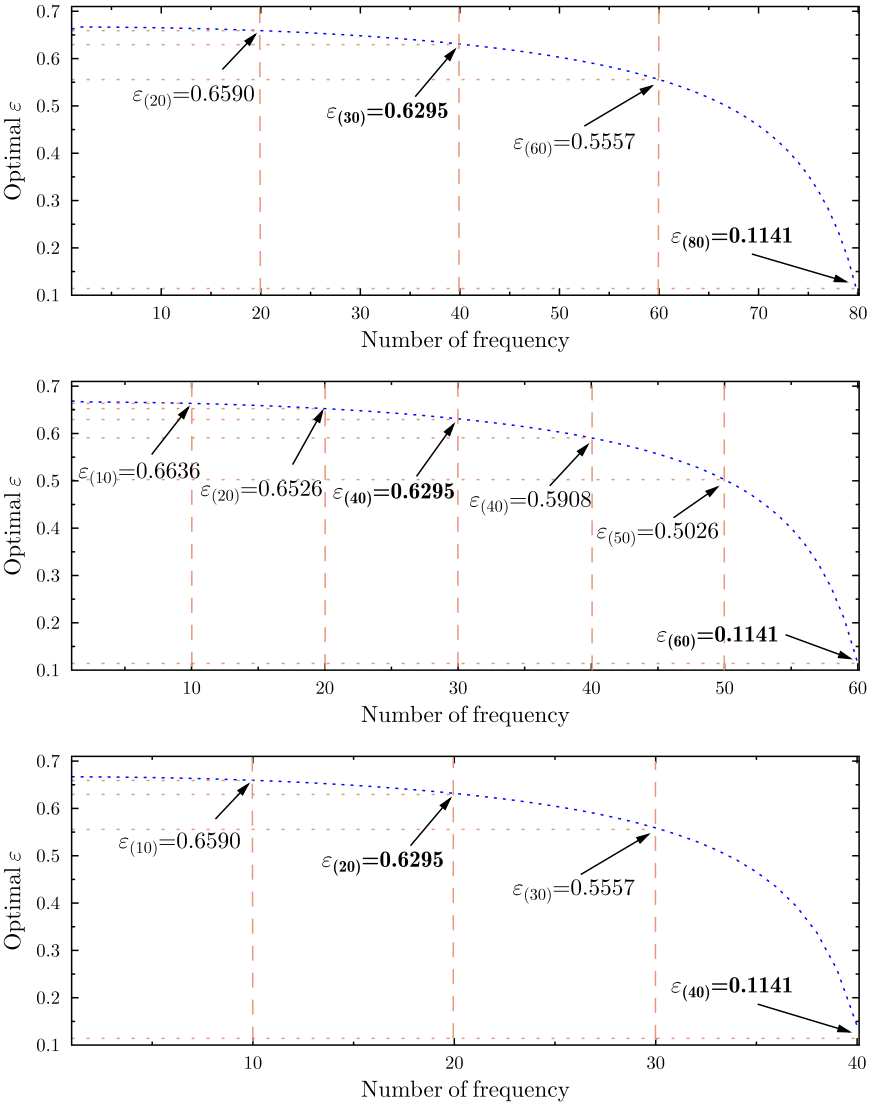

Figure 9: The ε coefficient for specific natural frequencies - three-node finite element.

Comparing the first, positive, non-zero root of the eigenproblem with the relation describing the first natural frequency of longitudinal vibrations of the rod, determined analytically, a value of $\varepsilon = 0.3517$ was obtained. The same value of ε was also obtained for the free-free and fixed-fixed rods. Finally, the mass matrix for the four-node rod finite element has been assumed as the following relation:

$$M_e = \frac{\rho AL}{1680}\begin{bmatrix} 128 & 99 & -36 & 19 \\ 99 & 648 & -81 & -36 \\ -36 & -81 & 648 & 99 \\ 19 & -36 & 99 & 128 \end{bmatrix}(1-\varepsilon) + \frac{\rho AL}{194}\begin{bmatrix} 16 & 0 & 0 & 0 \\ 0 & 81 & 0 & 0 \\ 0 & 0 & 81 & 0 \\ 0 & 0 & 0 & 16 \end{bmatrix}\varepsilon. \tag{35}$$

5.1. Numerical calculations

Similarly as in the case of two- and three-node elements, the relative error values for the natural frequencies of the rod modeled with 60 four-node elements have been first determined. Additionally, the same material and geometrical

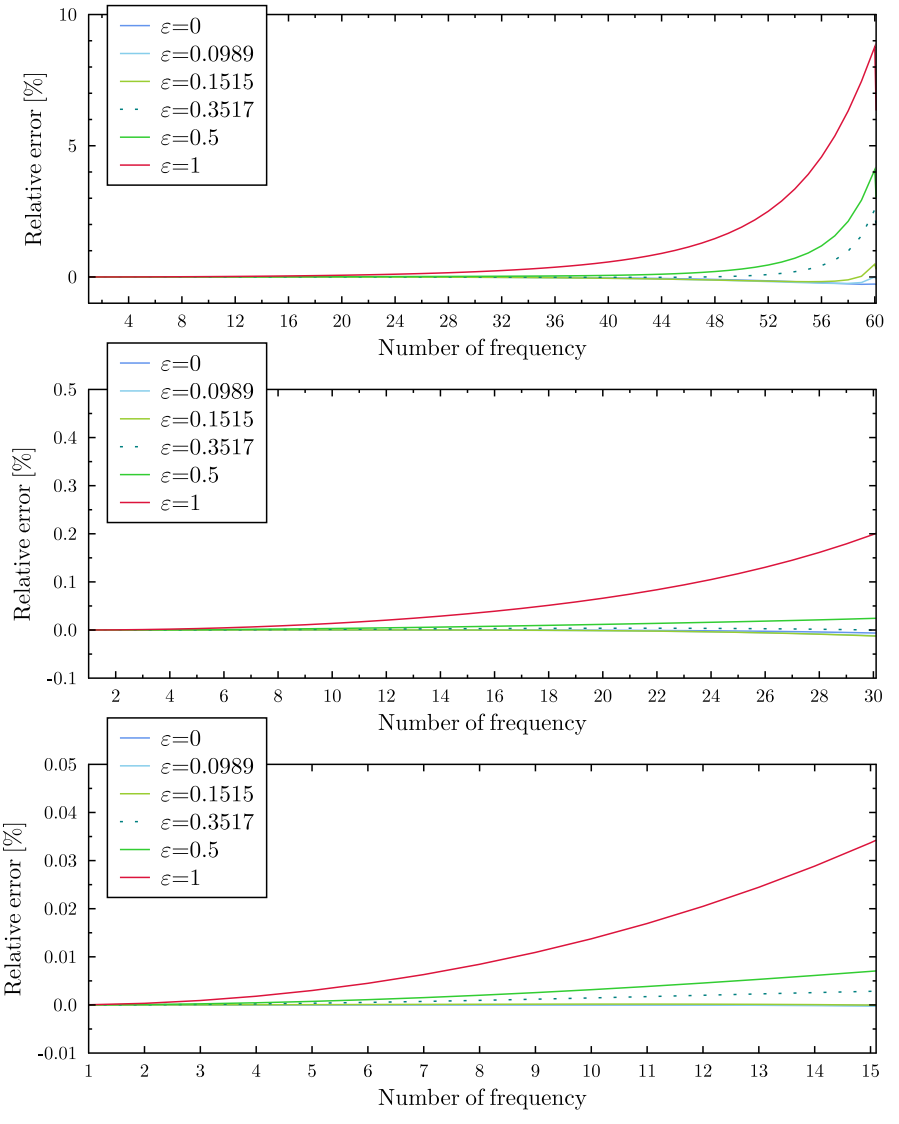

Figure 10: Relative error of the natural frequency determination of a fixed-free rod - 60, 30 and 15 four-node finite elements.

parameters used for the calculations presented earlier in this paper have been assumed. The relative error of the natural frequency has been determined according to the relation given in Eq.29. The results of the error calculations have been presented in Fig.10. The top graph shows the changes in the error values calculated for the whole frequency range. The middle and bottom graphs show the changes in error values calculated for half and quarter of the analyzed frequency spectrum, respectively. From the presented figures it can be seen that the value of the relative error significantly depends on the number of calculated frequencies. Moreover, small values of errors appear for different values of ε, therefore the optimal value of this parameter should be determined by subsequent numerical analyses.

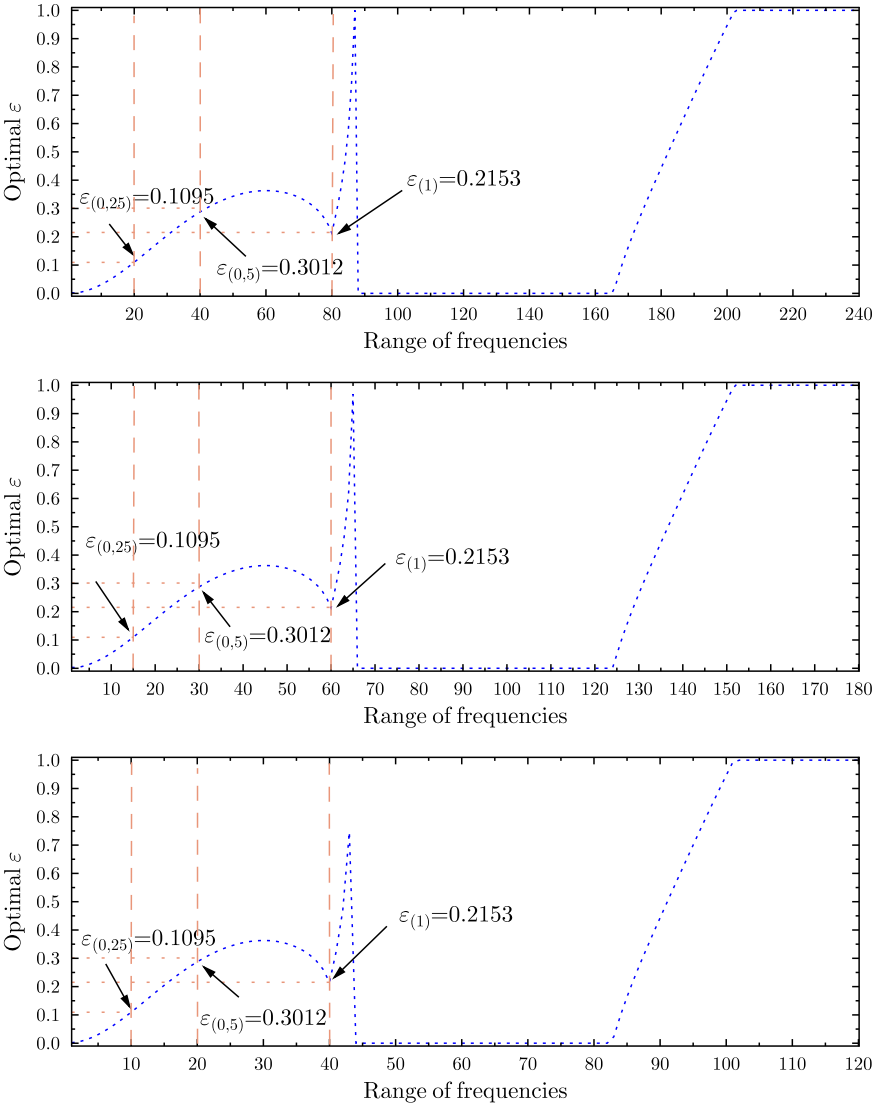

Figure 11: The ε coefficient for the natural frequency ranges of the analyzed rod - 80, 60 and 40 four-node finite elements.

Table 5
Average errors for 4-node element as a function of ε calculated for different ranges of frequencies

Range	ε=1.0	ε=0.0	ε=**0.2153**	ε=**0.3012**	ε=**0.1095**
Full	1.071	0.0536	**0.0506**	0.0875	0.0574
Half	0.0574	0.0013	0.0018	**0.0010**	0.0022
Quarter	0.0116	5.16e-05	0.0008	0.0022	**1.62e-5**

Considering the findings presented above, the calculation of the optimal value of the ϵ parameter for the rod modelled with a varied number of four-node elements (i.e., 40, 60, and 80) has been carried out, as in the case of the two-node and three-node elements. The results of these calculations have been shown in Fig.11. In this figure, as in the case of the analysis for two- and three-node finite elements, the red dashed lines indicate the Nyquist, half Nyquist, and one-quarter Nyquist frequencies for each of the analyzed cases. It is worth explaining at this point that in all figures a discontinuity can be observed in the one-third and two-third bandwidths of the analyzed spectra. This effect, as in the model using three-node elements, appears due to the periodic nature of the model Żak et al. (2016), so the common belief that any numerical model allows the determination of as many natural frequencies as its number of DOFs can be misleading in certain cases. Nevertheless, the values of ϵ for which the average error of the various ranges of frequencies have been calculated have been determined and those results have been presented in Table 5.

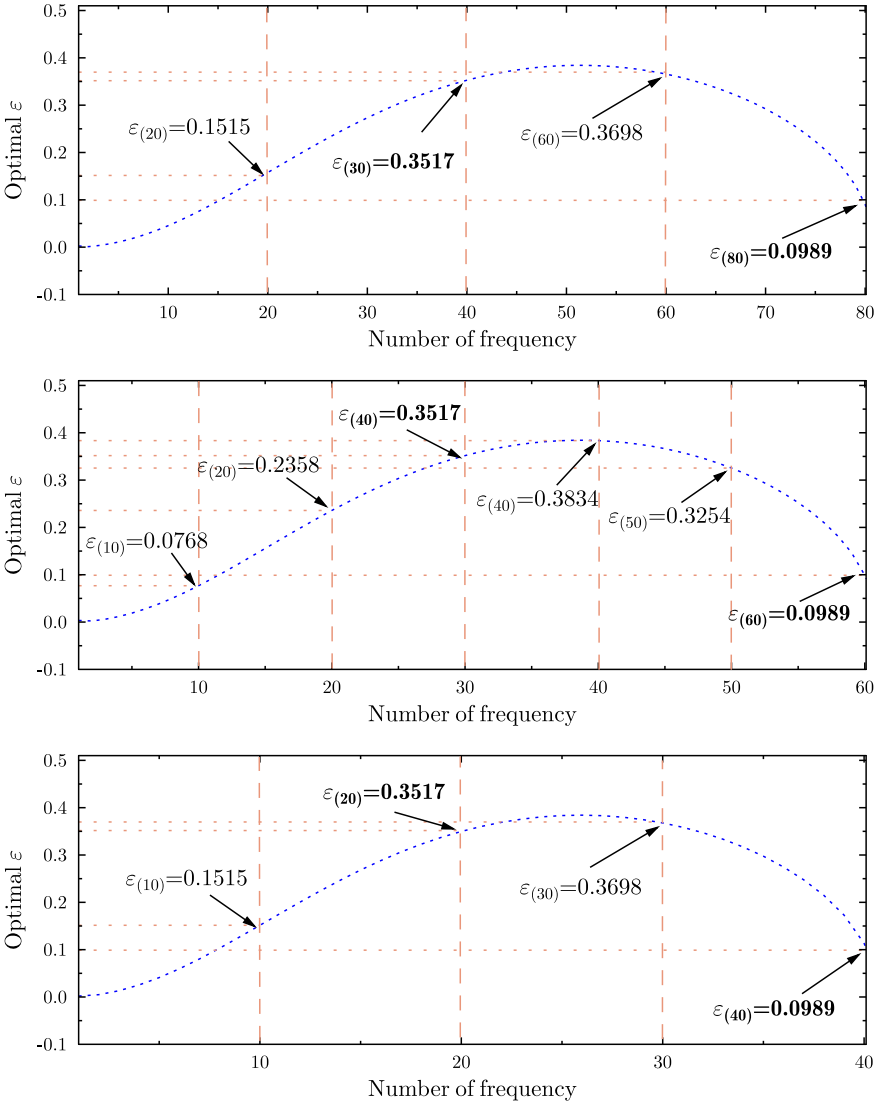

Figure 12: The ϵ coefficient for specific natural frequencies - four-node finite element.

Taking into account the above results, the authors have continued to attempt to answer the question of what is the optimal value of the ϵ factor from the point of view of minimizing the error in the determination of the natural frequencies for a model using a four-node element. For this purpose, calculations of the optimal value of the coefficient

ε for each frequency of the spectrum have been carried out (Fig.12). Similarly to the results obtained for the two-node and three-node models, it can be concluded from the curves shown in Fig.12 that the optimal value of ε has not been affected by the total number of finite elements in the model. For the full frequency spectrum, the best correlation between the analytical and numerical solutions has been obtained for $\varepsilon = 0.0989$. For half of the spectrum, the optimal value of ε is equal to 0.3517, while for the quarter of the spectrum $\varepsilon = 0.1515$. It was also found that the value of ε did not change for different types of boundary conditions, so, as in the previous subsections, the overview figure has been omitted.

Table 6
Relative errors as a function of ε calculated for specific frequency - 4-node finite element

No	ε=0.0	ε=0.0768	ε=0.2358	ε=0.3517	ε=0.3834	ε=0.3254	ε=0.0989
1	**3.46e-11**	2.15e-07	2.04e-06	4.54e-06	5.39e-06	3.88e-06	3.58e-07
10	-7.44e-06	**1.26e-07**	0.00056	0.00145	0.00176	0.00122	3.46e-05
20	-0.00054	-0.0013	**2.99e-06**	0.0037	0.00510	0.00266	-0.0014
30	-0.00619	-0.01099	-0.01000	**9.90e-06**	0.00411	-0.00294	-0.01174
50	-0.03336	-0.04721	-0.04310	-0.01239	**4.05e-05**	-0.02140	-0.04928
40	-0.11828	-0.14500	-0.09227	0.03555	0.08310	**0.00013**	-0.14636
60	-0.27121	-0.16669	1.3549	2.56919	2.89806	2.29486	**0.00063**

The observations described above have been confirmed by the results gathered and presented in Table 3. The table presents a set of values of calculated relative errors for selected frequencies in the case of specified values of the ε parameter. The smallest values of the calculated errors have been marked in bold text (on the diagonal) - as it can be easily noticed, these are the results for certain optimal values of ε (listed in the first row of the table), what is additionally marked in the middle graph of Fig12.

6. Conclusions

The main objective of the research described in this paper has been to determine the optimal mass matrix for a rod finite element, with the purpose of improving the accuracy of eigenvalue calculations. It has been assumed that the matrix can be structured as a linear combination of coherent and diagonal mass matrices by using a certain weight factor. In order to determine the optimal value of this factor, the eigenvalues of the discrete model have been compared with the analytical values. From this, the optimal weight coefficients for the two-, three- and four-node rod finite elements have been determined.

Based on the literature review, it has been found that certain values of weighting coefficients exist, however, their application is limited only to the lowest ranges of rod natural frequencies, since, according to the literature sources cited in this paper, only in the low range are the errors at an acceptable level. The use of previously known coefficients leads to an increase in the error value with an increase in the range of the determined natural frequencies. This phenomenon is numerically harmful, therefore, an attempt has been made to develop such a coefficient, which allows the analysis of rod natural vibrations with minimum numerical errors for both low and high natural frequencies. Therefore, this paper presents new forms of the mass matrix of a rod element which allows one to determine natural frequencies with the smallest average error for a specific range of frequencies or with the smallest relative error for a specific number of frequencies.

During numerical investigations, it has been found that in the case of the two-node element analysis for the first natural frequencies, the best results may be obtained for $\varepsilon = 0.5$ - that is for the so-called superconvergent mass matrix built on the basis of trigonometric polynomials Ahmadian and Faryghi (2011). However, if one would like to determine the longitudinal natural frequencies from the whole spectrum with the smallest possible mean error (up to the Nyquist frequency), whose number is related to the number of DOFs of the model, $(N-1)/2$, the best results can be obtained using $\varepsilon = 0.4604$. The optimal ε value for the Nyquist frequency is then 0.4317. Similarly, for the three-node element for the first natural frequencies, the smallest error is obtained at $\varepsilon = 2/3$, while for the whole frequency range up to the Nyquist frequency for $\varepsilon = 0.4301$. For the half frequency, $\varepsilon = 0.6295$. In the case of the four-node element, for the first natural frequencies, the smallest error is obtained at $\varepsilon = 0$, while for the whole frequency range up to the Nyquist frequency for $\varepsilon = 0.3012$. For the half frequency - $\varepsilon = 0.3517$.

From analyzing the results of the performed tests, it has been concluded that it is not possible to determine the optimal value of the weighting factor ϵ for the entire frequency range. Nevertheless, it is possible to find such coefficients that for the selected frequency range will give the smallest average error. Furthermore, for a certain number of frequencies, there is a weighting factor that gives a smaller error. It has also been found that the weighting factors do not depend on the grid density or on the boundary condition type.

CRediT authorship contribution statement

Marek Krawczuk: Conceptualization of this study, Methodology, Software. **Magdalena Palacz:** Software, Data curation, Writing - Original draft preparation.

References

Ahmadian, H., Faryghi, S., 2011. Shape functions of superconvergent finite elements. Thin-Walled Structures 49, 1178–1183.

Beslin, O., Nicolas, J., 1997. A hierarchical functions set for predicting very high order plate bending modes with any boundary conditions. Journal of Sound and Vibration 202, 633–655.

Dokumaci, E., 2006. On superaccurate finite elements and their duals for eigenvalue computation. Journal of Sound and Vibration 298, 432–438.

Doyle, J., 1997. Wave Propagation in Structures. Spectral Analysis Using Fast Discrete Fourier Transforms, 2nd ed. Springer.

Fried, I., Chavez, M., 2004. Superaccurate finite element eigenvalue computation. Journal of Sound and Vibration 275, 415–422.

Hashemi, S., 2004. The use of trigonometric interpolation functions for vibration analysis of beam structures - bridging gap between fem and exact formulations. Transactions on the Built Environment vol 71, © 2004 WIT Press 71, 197–206.

Kim, K., 1993. A review of mass matrices for eigenproblems. Computers and Structures 46, 1041–1048.

Ostachowicz, W., Kudela, P., Krawczuk, M., Żak, A., 2012. Guided Waves in Structures for SHM: The Time-Domain Spectral Element Method. Wiley & Sons, West Sussex, UK.

Palacz, M., 2018. Spectral methods for modelling of wave propagation in structures in terms of damage detection — a review. Applied Sciences 8, 1–25.

Patera, A., 1984. A spectral element method for fluid dynamics: Laminar flow in a channel expansion. Journal of Computational Physics 54, 468–488.

Stavridis, C., Clinckemailier, J., Dubois, J., 1989. New concept for finite element mass matrix formulations. AiAA Journal 27, 1249–1255.

Żak, A., Krawczuk, M., Palacz, M., 2016. Periodic properties of 1d fe discrete models in high frequency dynamics. Mathematical Problems in Engineering 2016, 1–15.

Zboiński, G., 2010. Adaptive hpq finite element methods for the analysis of 3d-based models of complex structures. part 1. hierarchical modeling and approximations. Computer Methods in Applied Mechanics and Engineering 199, 2913–2940.

Zboiński, G., 2013. Adaptive hpq finite element methods for the analysis of 3d-based models of complex structures. part 2. a posteriori error estimation. Computer Methods in Applied Mechanics and Engineering 267, 531–565.

Zienkiewicz, O., Taylor, R., 1989. The finie element method. McGraw-Hill, New York.